



**International Global Navigation Satellite Systems Society
IGNSS Symposium 2007**

The University of New South Wales, Sydney, Australia
4 – 6 December, 2007

Performance Analysis Of An Integrated Navigation System In Urban Canyon Environment

Ben K.H. Soon

Australian Centre for Field Robotics (ACFR)
Centre for Autonomous Systems (CAS)
The University of Sydney, Australia

Tel: +61-2-90366452 Fax: +61-2-93517474 Email: b.soon@acfr.usyd.edu.au / skahhol@dso.org.sg

S. Scheduling

Australian Centre for Field Robotics (ACFR)
Centre for Autonomous Systems (CAS)
The University of Sydney, Australia

Tel: +61-2-93518929 Fax: +61-2-93517474 Email: s.scheduling@acfr.edu.au

H.K. Lee

School of Electronics, Telecommunication & Computer
Hankuk Aviation University, Republic of Korea
Email: hyklee@mail.hangkong.ac.kr

H.K. Lee

Department of Civil Engineering
Changwon National University, Republic of Korea
Email: hkyulee@changwon.ac.uk

H. Durrant-Whyte

Australian Centre for Field Robotics (ACFR)
Centre for Autonomous Systems (CAS)
The University of Sydney, Australia

Tel: +61-2-93515583 Fax: +61-2-93517474 Email: hugh@acfr.usyd.edu.au

ABSTRACT

Motivated by the requirements to provide continuous accurate navigation solution to bridge the periods when there is a decreased in the availability of GPS satellites or/and distinctive landmarks operating in an urban canyon environment (e.g. DARPA Urban Challenge 2007) or integrated *pseudo* Simultaneous Localization And Mapping system (*p*SLAM) in a cluttered environment (Soon *et al.*, 2006). This paper describes a simple and effective approach that incorporates standalone time differenced GPS L1 carrier phase (TDCP) measurements and vehicle dynamic constraints to aid INS in an urban canyon environment. The formulation of the TDCP observation model is described in tightly coupled GPS/INS iterative extended Kalman filter (IEKF) approach (Soon *et al.*, 2007). Land vehicle trial was conducted to analyse the accuracy performance of the integrated navigation system in an urban canyon environment.

KEYWORDS: IEKF, TDCP, Tightly-Coupled, INS, ZUPT

1. INTRODUCTION

With full operational GPS capability, it has been recognized that GPS and inertial navigation systems have complimentary features which can be exploited in an integrated system to create synergistic improvements in navigation performance. The estimates of INS error parameters allow GPS/INS navigation with substantially smaller errors than could be achieved with either a standalone inertial or GPS navigation (Cox, 1978). Techniques like carrier-smoothed code differential (Hofmann-Wellenhof *et al.*, 2001) (Lee *et al.*, 2004b) or ambiguity resolution (Hatch, 1990) (Chen, 1994) (Teunissen *et al.*, 1994) can be applied and result in positioning accuracy in the order of centimetre or better. Usually differential corrections are required in order to exploit the high accuracy of the carrier phase measurements, to enhance standalone GPS performance. Differential techniques using carrier phase processing for accurate estimation in general are time consuming and involve complication especially for single frequency receivers (Lee, 2004a). Integer resolution techniques, while ingenious and often successful, carry disadvantages that can seriously compromise overall success. Potential problems include delays that can disrupt real-time operation (e.g. the requisite geometric diversity needed in (re)acquisition of satellites, plus shorter pauses for mini-search in acquisition), or temporary false indications of ambiguity resolution, producing errors far beyond acceptable design limits (Farrell, 2001). Furthermore in an environment in which GPS signals are lost and reacquired frequently or availability/continuity of DGPS service within the area of operation is not guaranteed, ambiguity resolution is often not possible.

Another potential usage of the carrier phase measurements in a single receiver autonomous mode is by carrier-smoothing of the noisy-code measurements (Hofmann-Wellenhof *et al.*, 2001). However, the effectiveness of the phase-smoothing technique is limited because in a kinematic environment, frequent signal outages occur and every time this happens, all of the smoothed pseudorange information is lost and the accuracy of the pseudorange reverts back to its nominal unsmoothed-noisy level and the smoothing process has to be reinitialized. An alternative technique for generating navigation solution is with the use of velocity model. Doppler measurements can be used to estimate average velocity. This approach helps maintain position accuracy when the constellation drops below four satellites, and also helps reduce the effect of pseudorange errors when the number of satellites is four or more. But the Doppler measurement measures only average velocity so some assumptions about the system

dynamics must be made. This adds the requirement of additional system noise in the positioning filter, which reduces its accuracy (Ford *et al.*, 2003). It is known that velocities determined through the use of carrier-phase derived Doppler measurements are more accurate than the application of Doppler measurements (Moafipour *et al.*, 2004).

This paper investigates a filter update technique based on time differenced carrier phase measurements in the tightly-coupled GPS/INS system using iterative extended Kalman filter (IEKF), to assure availability and continuity of the navigation solution in an urban canyon environment. TDCP measurements provide precise position change between two epochs without using any ambiguity resolution techniques. In addition, land vehicle dynamic constraints are included in the estimation. The system performance will be investigated by using land vehicle test data collected in an urban-canyon environment.

2. TIME-DIFFERENCED CARRIER PHASE (TDCP) MEASUREMENT MODEL – ‘SATELLITE ODOMETRY’

In this section, a simple approach is described which allows to benefit from the carrier phase measurements without the need of differential corrections being transmitted from a base station and ambiguity resolution techniques. The basic method is to form time differenced successive carrier phase measurements to the same satellite; a user position difference is directly observable. This eliminates the constant integer ambiguities, N and most of the common mode errors, as they vary slowly with time. Triple differenced carrier phase measurements are already used in many applications, for estimation of GPS velocity which is independent of ambiguity terms (Moafipour *et al.*, 2004) and mostly for detection of cycle slips. Triple differenced measurements are obtained by first forming differences between the measurements of a base station and a rover, second between different satellites and finally between two successive epochs.

With the approach described here, only differences between two successive carrier phase measurements at t_k and t_{k-1} , respectively are formed. The advantage of this approach over carrier smoothed code is that, for the filter to make use of the TDCP measurements, it need only be available since the previous time epoch, rather than over the last 50 or so. Provided that some selection of four satellites is available over every epoch, the position accuracy of the system can be maintained and improved. This is in contrast to the carrier smoothed code technique, in which the same four satellites must be continuously tracked for the position accuracy to be maintained and improved by the same amount. In certain environments, various satellites are obstructed periodically. In some cases, the minimum number of satellites may be available for a solution all the time, but it is possible for the tracking duration for all the satellites to be short. In this environment, carrier smoothing the pseudorange is of little help because none of the individual satellites are tracked long enough to reduce the uncertainty for the carrier-smoothed measurements. Intuitively, enough information should be available from TDCP measurements so that the epoch-to-epoch position change can be determined to the level of the TDCP accuracy provided at least four delta carrier measurements are available.

Figure 1 shows the relative GPS satellite/vehicle geometry at two successive epochs. Time differenced carrier phase measurement (in cycles) can be formulated as follows using Eq. (1):

$$\begin{aligned}
\Delta\Phi &= \Phi_{t_k} - \Phi_{t_{k-1}} \\
&= [\lambda^{-1}(r - I_\phi + T_\phi) + \frac{c}{\lambda}(dt_{u_b} - dt_s) + N + \varepsilon_\phi]_{t_k} - \\
&\quad [\lambda^{-1}(r - I_\phi + T_\phi) + \frac{c}{\lambda}(dt_{u_b} - dt_s) + N + \varepsilon_\phi]_{t_{k-1}} \\
&= \lambda^{-1}(r_{t_k} - r_{t_{k-1}}) + \frac{c}{\lambda}(dt_{u_b,t_k} - dt_{u_b,t_{k-1}}) + \varepsilon_{\Delta\Phi} \\
&= \lambda^{-1}\Delta r + \frac{c}{\lambda}dt_{u_d} + \varepsilon_{\Delta\Phi}
\end{aligned} \tag{1}$$

where Φ is the measured carrier phase in cycles; r is the geometric range between the user position and the satellite position; λ is the wavelength; c is the speed of light; I_ϕ is the ionospheric error; T_ϕ is the tropospheric error; dt_{u_b} is the user clock bias; dt_s is the satellite clock error; N is the integer ambiguity and Δr is change in geometric range between two measurement epochs; dt_{u_d} is the user clock drifts and the remaining measurement error that is not removed by forming time differences is denoted with $\varepsilon_{\Delta\Phi}$ which is the residual error due to change in errors in the satellite clock, satellite position, ionospheric, tropospheric, multipath and receiver noise between epochs and are considered to be negligible.

Using time differenced of the carrier phase measurements from two consecutive epochs eliminates the integer ambiguity, N and common mode errors which allow direct estimation of precise differenced in user position – alternatively it is known as ‘*satellite odometry*’ in this research. Atmospheric delay compensations are not required in this simple processing procedure. Ionospheric and tropospheric delay changes are not compensated using dual-frequency measurements and high-fidelity tropospheric model to mitigate the influence of changes in tropospheric delay respectively. The integers remain fixed as long as the carrier tracking loop maintains lock. Momentary loss of phase lock can result in a discontinuity in the integer cycle even though the fractional part of the phase is measured continuously. Such discontinuity in the integer cycle count is called a cycle slip. The constant integer phase ambiguity is removed completely and an estimation of this quantity using carrier differential techniques like RTK is not necessary.

From Eq. (1), the change in geometric range between two epochs (in metre) can be represented as (Soon *et al.*, 2007):

$$\begin{aligned}
\Delta\Phi &= \left[\left| \mathbf{r}_{SV,t_k} - \mathbf{r}_{u,t_k} \right| - \left| \mathbf{r}_{SV,t_{k-1}} - \mathbf{r}_{u,t_{k-1}} \right| \right] + cdt_{u_d} + \varepsilon_{\Delta\Phi} \\
&= \left[\mathbf{I}_{t_k} \bullet (\mathbf{r}_{SV,t_k} - \mathbf{r}_{u,t_k}) - \mathbf{I}_{t_{k-1}} \bullet (\mathbf{r}_{SV,t_{k-1}} - \mathbf{r}_{u,t_{k-1}}) \right] + cdt_{u_d} + \varepsilon_{\Delta\Phi}
\end{aligned} \tag{2}$$

where \mathbf{r}_{SV} is the GPS satellite position vector, \mathbf{r}_u is the user position vector, dt_{u_d} is the user clock drifts and \mathbf{I} is the unit vector pointing to the satellite from the user position.

From the TDCP measurement model, the current measurement at time t_k is linearly connected to the $\mathbf{r}_{u,t_{k-1}}$, previous user position state as well as the current one \mathbf{r}_{u,t_k} , and this violates the format of the usual Kalman filter model (Brown *et al.*, 1969). In practice, various approximations have been used to accommodate the delayed-state term. The work of Soon *et*

al. (2007) to handle the delayed-state measurement problem is used in this research.

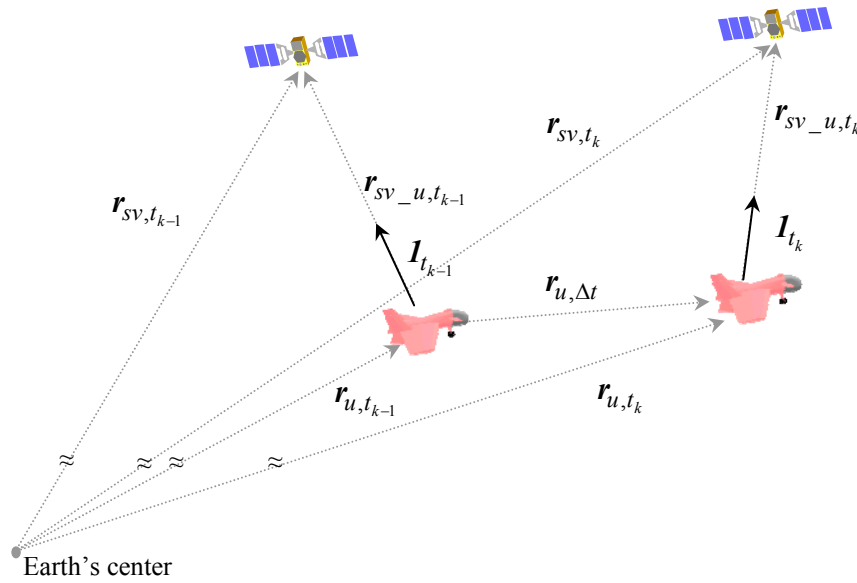


Figure 1. Relative GPS satellite/vehicle geometry at two successive epochs.

Stochastic characteristics of empirical TDCP measurements in static condition shows that over a 10-minute period the mean of the residual is generally closed to zero at 0.1-0.4 mm level indicating the TDCP measurement model is an adequate model and the standard deviations are on the order of 1.0-3.0 mm which are dependent on satellite elevations (Soon *et al.*, 2007).

3. LAND VEHICLE DYNAMIC CONSTRAINTS – ZERO VELOCITY UPDATE (ZUPT) AND AUXILIARY MEASUREMENT UPDATE

Operating in urban canyon environments often results in complete and partial GPS outages of varying durations, which can be addressed in a tightly-coupled GPS/INS mode when less than 4 satellites are available however the position error drifts are not observable in all directions. To further improve the navigation system performance, the use of several land vehicle dynamic constraints is proposed in this section. In stationary case, static INS calibration which commonly known as Zero Velocity Update (ZUPT) mode should be supported. Periodic ZUPTs should be automatically requested by the system's controls or at each traffic stop, depending on the level of positioning error growth. Though ZUPT provides an alternative to calibrate the inertial system when there are frequent GPS outages, this mode of operation only allows an improved calibration of velocity error sources, such as alignment and the IMU sensor errors, leading to the lower positioning error rate as compared to the unaided, free navigation mode.

In kinematic case, land vehicles are sometimes modeled kinematically with assumptions of zero lateral velocity, no wheel slip and the existence of a direct relationship between steer angle and yaw rate - non-holonomic constraints. At low speeds, these assumptions may be valid. At higher speeds or on varying terrains, these assumptions quickly break down resulting in undesired performance from navigation and/or control algorithms. Lateral velocities are generated and the vehicle sideslip becomes large enough to impact the system

and it cannot be assumed negligible. Vehicle sideslip is formally defined as the angle between the vehicle's heading vector and the vector that denotes the vehicle's actual path of travel. High speed is also a term that is particular to each vehicle and the ground it is traversing. Terrain is a critical factor that drastically changes the available peak forces of the tire, which are located in the nonlinear region of the tire curve. This too, can change the relative meaning of the term high speed.

A series of 'Figure-of-8' manoeuvres as shown in Figure 2, were executed on the landing strip at The University of Sydney's trial site at Marulan, Sydney using the Toyota 4WD Land Cruiser. The vehicle's speed was approximately 12 m/s (43 km/h) on the straight sections and slowed down to 5 m/s (18 km/h) when approached the turnings. NovAtel SPAN system operating in RTK mode was used to estimate the vehicle velocity vector in body-frame as seen in Figure 3. The results show that the lateral velocity, v_y^b is approximately zero while the vehicle was travelling straight however when approaching each turn the velocity increases to about 0.5 m/s due to sideslip, which violates the assumption that lateral velocity can be estimated zero. Another observation from the plots is the vertical velocity, v_z^b is approximately zero throughout the series of manoeuvres. This assumption can be used as an auxiliary velocity update when there are outages in GPS. In addition, another constraint that can be introduced in a land vehicle environment is through a height measurement. Measurements can be derived from the fact that the height changes slowly in land vehicle environments.

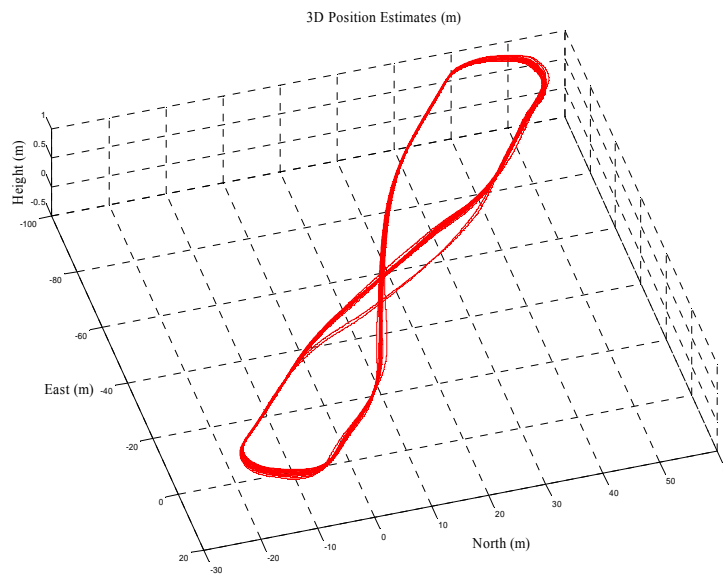


Figure 2. Overview of the driving manoeuvres on the landing strip.

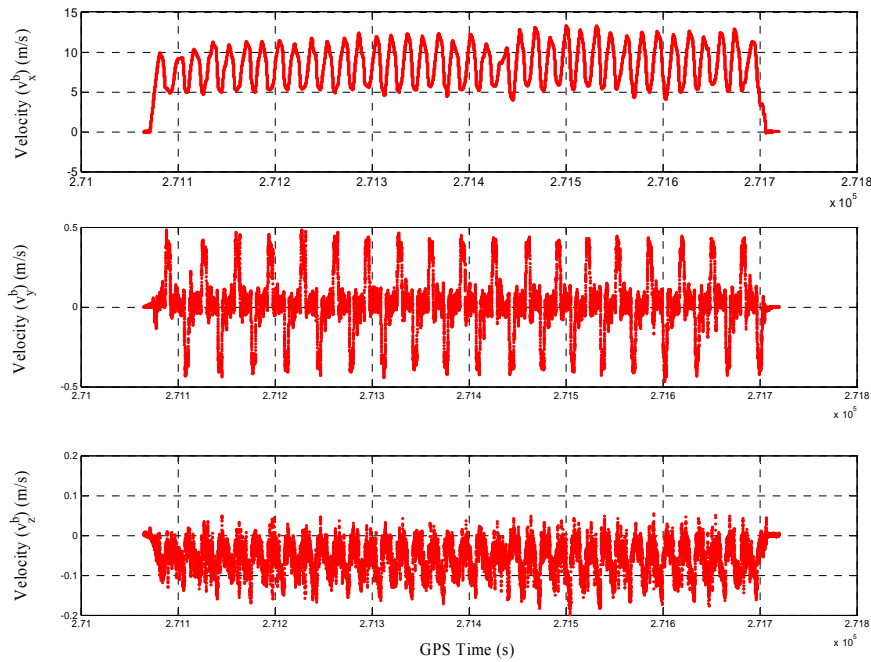


Figure 3. Estimated vehicle velocities (*body-frame*).

4. INTEGRATED INS/TDCP/ZUPT ITERATIVE EXTENDED KALMAN FILTER (IEKF) DESIGN

In this paper, a tightly-coupled integration architecture, where TDCP and inertial measurements are integrated using a single centralised 17-state iterative extended Kalman filter (IEKF) approach. The seventeen states are: position error (three states); velocity error (three states); inertial platform misalignment (three states); gyro drift rate (three states); accelerometer bias (three states) and user clock error (two states). To design the filter, the differential error model is specified and derived in this section. The dynamic model includes the mechanisation of the INS error states of position, velocity and attitude using the *Psi*-angle error approach augmented with the error states of IMU sensor biases and GPS receiver clock, whereas the measurement model is a linear relationship between the TDCP measurements and the error states. For land vehicle navigation applications, during ZUPT mode similar inertial error model is used.

INS Psi-Angle Error Model

Two dominant strapdown inertial navigation system error models have emerged in the literature: the *Psi*-angle (ψ -angle) and the *Phi*-angle (ϕ -angle) error models. Both models describe the same strapdown inertial navigation system errors in different frames of reference, they are equivalent. (Goshen-Meskin *et al.*, 1992) presented a unified approach to inertial navigation error modelling.

The ψ -angle error model is obtained from a linear perturbation analysis of the strapdown inertial navigation errors in the computer frame (*c-frame*), which is the navigation frame maintained by the inertial navigation system. The computer frame is a “known” reference frame, hence perturbations of the computer frame angular position and angular rate are zero.

This leads to a simpler model than the φ -angle error model.

$$\delta \dot{\mathbf{r}}_e^c = \delta \mathbf{v}_e^c - \boldsymbol{\omega}_{ec}^c \times \delta \mathbf{r}_e^c \quad (3)$$

$$\delta \dot{\mathbf{v}}_e^c = -(\boldsymbol{\omega}_{ic}^c + \boldsymbol{\omega}_{ie}^c) \times \delta \mathbf{v}_e^c + \nabla - \boldsymbol{\psi}^c \times \mathbf{f}^c + \delta \mathbf{g} \quad (4)$$

$$\dot{\boldsymbol{\psi}}^c = -\boldsymbol{\omega}_{ic}^c \times \boldsymbol{\psi}^c + \boldsymbol{\varepsilon} \quad (5)$$

where $\delta \mathbf{r}_e^c$, $\delta \mathbf{v}_e^c$ and $\boldsymbol{\psi}^c$ are the velocity, position and attitude error vectors respectively; ∇ , the accelerometer error vector; $\delta \mathbf{g}$, the error in the computed gravity vector; $\boldsymbol{\varepsilon}$, the gyro drift vector; \mathbf{f}^c , the specific force vector sensed by the accelerometer in c -frame; $\boldsymbol{\omega}_{ec}^c$, the angular rate of the c -frame with respect to the earth; $\boldsymbol{\omega}_{ie}^c$, the angular rate of the earth with respect to inertial space and $\boldsymbol{\omega}_{ic}^c = \boldsymbol{\omega}_{ie}^c + \boldsymbol{\omega}_{ec}^c$, the angular rate of the c -frame with respect to the inertial space.

GPS Receiver Clock Error Model

A basic 2-state model is commonly used in most Kalman filter implementations allows for the estimation of both clock bias and drift, representing the dominant error source associated with the GPS measurements. Numerical values for the spectral densities of the white noise forcing functions depend on the quality of the crystal clock. Besides the receiver clock error model, filter designers have also been concerned with the errors in the pseudorange and carrier phase measurements to each satellite due to residual satellite clock and orbit errors, transmission path effects (atmospheric errors) and tracking loop errors. Inclusion of an error state for each of these measurements can obtain a calibration of the measurement under certain conditions.

The differential clock model is (Brown *et al.*, 1997):

$$\begin{bmatrix} dt_{u_b} \\ dt_{u_d} \end{bmatrix} = \begin{bmatrix} 0 & 1 \\ 0 & 0 \end{bmatrix} \begin{bmatrix} dt_{u_b} \\ dt_{u_d} \end{bmatrix} + \begin{bmatrix} w_{u_b} \\ w_{u_d} \end{bmatrix} \quad (6)$$

Integrated INS/TDCP Error Dynamic Model

The 17-state error dynamic model is represented as:

$$\begin{aligned}
 \begin{bmatrix} \delta \dot{r}_e^c \\ \delta \dot{v}_e^c \\ \dot{\psi}^c \\ \delta \dot{f}^b \\ \delta \dot{\omega}^b \\ \dot{dt}_{u_b} \\ \dot{dt}_{u_d} \end{bmatrix} &= \begin{bmatrix} (-\omega_{ec}^c \times) & \mathbf{I}_{3 \times 3} & \mathbf{0}_{3 \times 3} & \mathbf{0}_{3 \times 3} & \mathbf{0}_{3 \times 3} & 0 & 0 \\ \mathbf{F}_{21} & [-(\omega_{ic}^c + \omega_{ie}^c) \times] & (\mathbf{f}^c \times) & \mathbf{C}_b^c & \mathbf{0}_{3 \times 3} & 0 & 0 \\ \mathbf{0}_{3 \times 3} & \mathbf{0}_{3 \times 3} & (-\omega_{ic}^c \times) & \mathbf{0}_{3 \times 3} & -\mathbf{C}_b^c & 0 & 0 \\ \mathbf{0}_{3 \times 3} & \mathbf{0}_{3 \times 3} & \mathbf{0}_{3 \times 3} & \mathbf{F}_{44} & \mathbf{0}_{3 \times 3} & 0 & 0 \\ \mathbf{0}_{3 \times 3} & \mathbf{0}_{3 \times 3} & \mathbf{0}_{3 \times 3} & \mathbf{0}_{3 \times 3} & \mathbf{F}_{55} & 0 & 0 \\ 0 & 0 & 0 & 0 & 0 & 0 & 1 \\ 0 & 0 & 0 & 0 & 0 & 0 & 0 \end{bmatrix} \begin{bmatrix} \delta r_e^c \\ \delta v_e^c \\ \psi^c \\ \delta f^b \\ \delta \omega^b \\ dt_{u_b} \\ dt_{u_d} \end{bmatrix} \\
 &+ \begin{bmatrix} \mathbf{0}_{3 \times 3} & \mathbf{0}_{3 \times 3} & \mathbf{0}_{3 \times 3} & \mathbf{0}_{3 \times 3} & 0 & 0 \\ \mathbf{C}_b^c & \mathbf{0}_{3 \times 3} & \mathbf{0}_{3 \times 3} & \mathbf{0}_{3 \times 3} & 0 & 0 \\ \mathbf{0}_{3 \times 3} & -\mathbf{C}_b^c & \mathbf{0}_{3 \times 3} & \mathbf{0}_{3 \times 3} & 0 & 0 \\ \mathbf{0}_{3 \times 3} & \mathbf{0}_{3 \times 3} & \mathbf{I}_{3 \times 3} & \mathbf{0}_{3 \times 3} & 0 & 0 \\ \mathbf{0}_{3 \times 3} & \mathbf{0}_{3 \times 3} & \mathbf{0}_{3 \times 3} & \mathbf{I}_{3 \times 3} & 0 & 0 \\ 0 & 0 & 0 & 0 & 1 & 0 \\ 0 & 0 & 0 & 0 & 0 & 1 \end{bmatrix} \begin{bmatrix} \mathbf{w}_\nabla \\ \mathbf{w}_\varepsilon \\ \mathbf{w}_{\nabla_b} \\ \mathbf{w}_{\varepsilon_b} \\ w_{u_b} \\ w_{u_d} \end{bmatrix}
 \end{aligned}
 \tag{7}$$

where the sub-matrices are expressed as:

$$\begin{aligned}
 \mathbf{F}_{21} &= \text{diag}[-g/R_e \quad -g/R_e \quad 2g/R_e] \\
 \mathbf{F}_{44} &= \text{diag}[-\tau_{\nabla_{b_x}} \quad -\tau_{\nabla_{b_y}} \quad -\tau_{\nabla_{b_z}}] \\
 \mathbf{F}_{55} &= \text{diag}[-\tau_{\varepsilon_{b_x}} \quad -\tau_{\varepsilon_{b_y}} \quad -\tau_{\varepsilon_{b_z}}]
 \end{aligned}$$

where \mathbf{C}_b^c , the direction cosine matrix from body frame (*b-frame*) to computer-frame (*c-frame*); $\mathbf{I}_{3 \times 3}$, a 3×3 identity matrix; $\mathbf{0}_{3 \times 3}$, a 3×3 zero matrix; R_e , Earth radius plus vehicle altitude; $\delta \mathbf{f}^b$, the accelerometer bias vector in *b-frame*; $\delta \boldsymbol{\omega}^b$, the gyro drift vector in *b-frame*; τ_{∇_b} and τ_{ε_b} are the time-constants for the first-order Gauss Markov processes of the accelerometer and gyroscope biases respectively and $\mathbf{w} = [\mathbf{w}_\nabla \quad \mathbf{w}_\varepsilon \quad \mathbf{w}_{\nabla_b} \quad \mathbf{w}_{\varepsilon_b} \quad w_{u_b} \quad w_{u_d}]^T$ are all zero-mean Gaussian white noise vectors.

5. TEST RESULTS

In this section, post-mission processing using the real-time algorithms is used to assess the integrated system performance. This research is conducted with real-time applications in mind. Though the algorithm was demonstrated in post-processing mode, no special pre-processing of the data was required. A series of tests were conducted to verify the performance of the approach to use TDCP and the auxiliary measurements to aid INS in an urban canyon environment. Without the availability of GPS base station within The

University of Sydney campus, the performance of the proposed navigation algorithm is compared with trajectories generated using raw GPS pseudorange measurements to aid the INS. The navigation system used for this research was a NovAtel SPAN system which contains a dual-frequency NovAtel ProPak-G2plus GPS receiver capable of tracking up to 12 satellites at a time and provides high-quality code, Doppler and carrier-phase measurements, interfaces with a tactical-grade Honeywell HG1700 AG17 IMU. Technical specifications of the IMU are provided in Table 1.

Table 1. Technical specifications of Honeywell HG1700 AG17/62 IMU.

Gyro Input Range	± 1000 deg/s
Gyro Rate Bias	5.0 deg/hr
Gyro Rate Scale Factor	150 ppm
Angular Random Walk	0.5 deg/ $\sqrt{\text{hr}}$
Accelerometer Range	± 50 g
Accelerometer Linearity	500 ppm
Accelerometer Scale Factor	300 ppm
Accelerometer Bias	2.0 mg

The IMU and GPS antenna were rigidly mounted onto the top of the trial vehicle, a Toyota HiLux Ute as shown in Figure 4. The lever-arm was estimated using the lever-arm calibration function available in the NovAtel SPAN system.

First test was performed in a ‘multipath-rich’ environment at the lower deck on the top level of the multi-storey car park at The University of Sydney as depicted in Figure 4, in order to demonstrate the effectiveness of the integrated system using only TDCP as updates. Without a truth trajectory to assess the accuracy performance, navigation data was collected by driving the vehicle in circles (locking the steering wheel), over duration of 200 s, which would ensure ‘repeatability’ in the circular trajectories. On average, 6-7 GPS satellites were tracked throughout the test.



Figure 4. The University of Sydney multi-storey car park.

The results of incorporating TDCP or pseudorange measurements in the tightly-coupled system can be seen by comparing the plots shown in Figure 5-6. It clearly shows that the integrated TDCP/INS solution is a much smoother and more accurate trajectory with a height error less than 0.2 m whereas the other solution shows fluctuations in the horizontal positions

and a height error of about 1.7 m, which is the result of noisy pseudorange measurements corrupted with multipath.

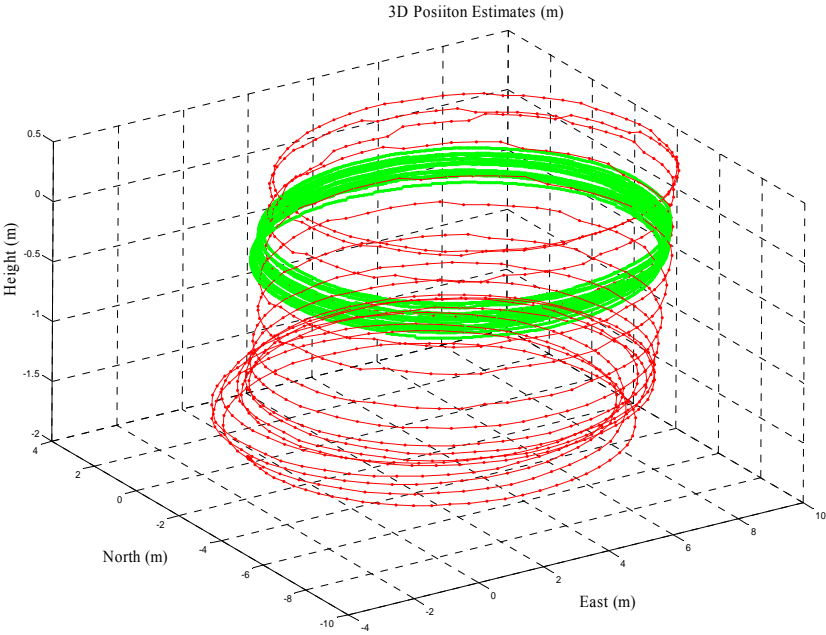


Figure 5. 3D vehicle circular trajectories (Tightly-coupled TDCP/INS solution (*Green*) and Tightly-coupled GPS/INS solution (*Red*)).

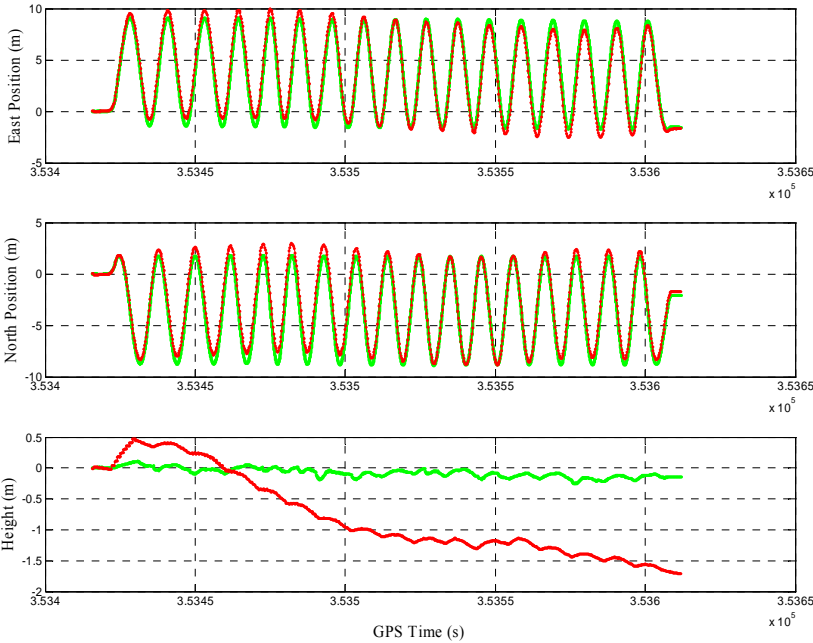


Figure 6. Position estimates from the dataset collected on the university multi-storey car park (Tightly-coupled TDCP/INS solution (*Green*) and Tightly-coupled GPS/INS solution (*Red*)).

The second kinematic test was conducted around the university campus. As discussed in the preceding section, the ZUPT mode at each traffic stop and the auxiliary measurement update when less than 4 satellites available are included in the estimation. The photograph (Google Earth) with over plot of the test trajectory in Figure 7 shows the tracking environment around

the university campus with significant masking due to tall buildings and heavy foliage along the streets which cause severe signal blockage, leading to frequent loss of lock. The least-squares – derived horizontal positions in Figure 8 shows that there are fewer than four satellites available for a significant proportion of the time. The least-squares trajectory also shows very noisy data and clearly demonstrates the effect of unchecked multipath errors. Maximum horizontal position error is approaching 30 m during certain portions of this dataset.



Figure 7. Test trajectory (Google Earth).

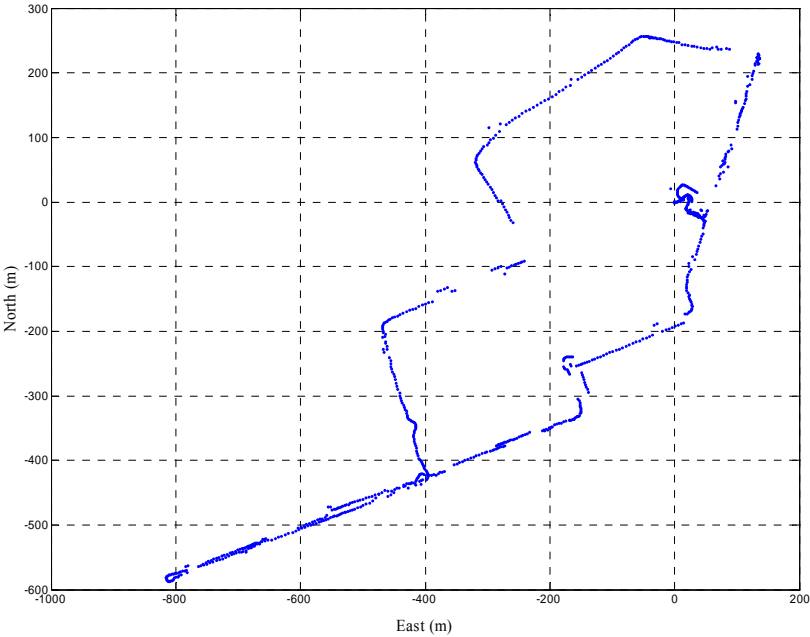


Figure 8. 2D vehicle trajectory as determined from GPS only least-squares solution.

Figure 9, trajectories of horizontal positions generated from both the tightly-coupled TDCP/INS and GPS/INS algorithms are shown. Both filters are able to bridge the portions of the test in which fewer than four satellites are in view. However, from various ‘zoomed in’ plots in Figure 9, show that the integrated TDCP/INS results is much smoother without any spikes in the position as compare to the other filter using raw pseudoranges as updates.

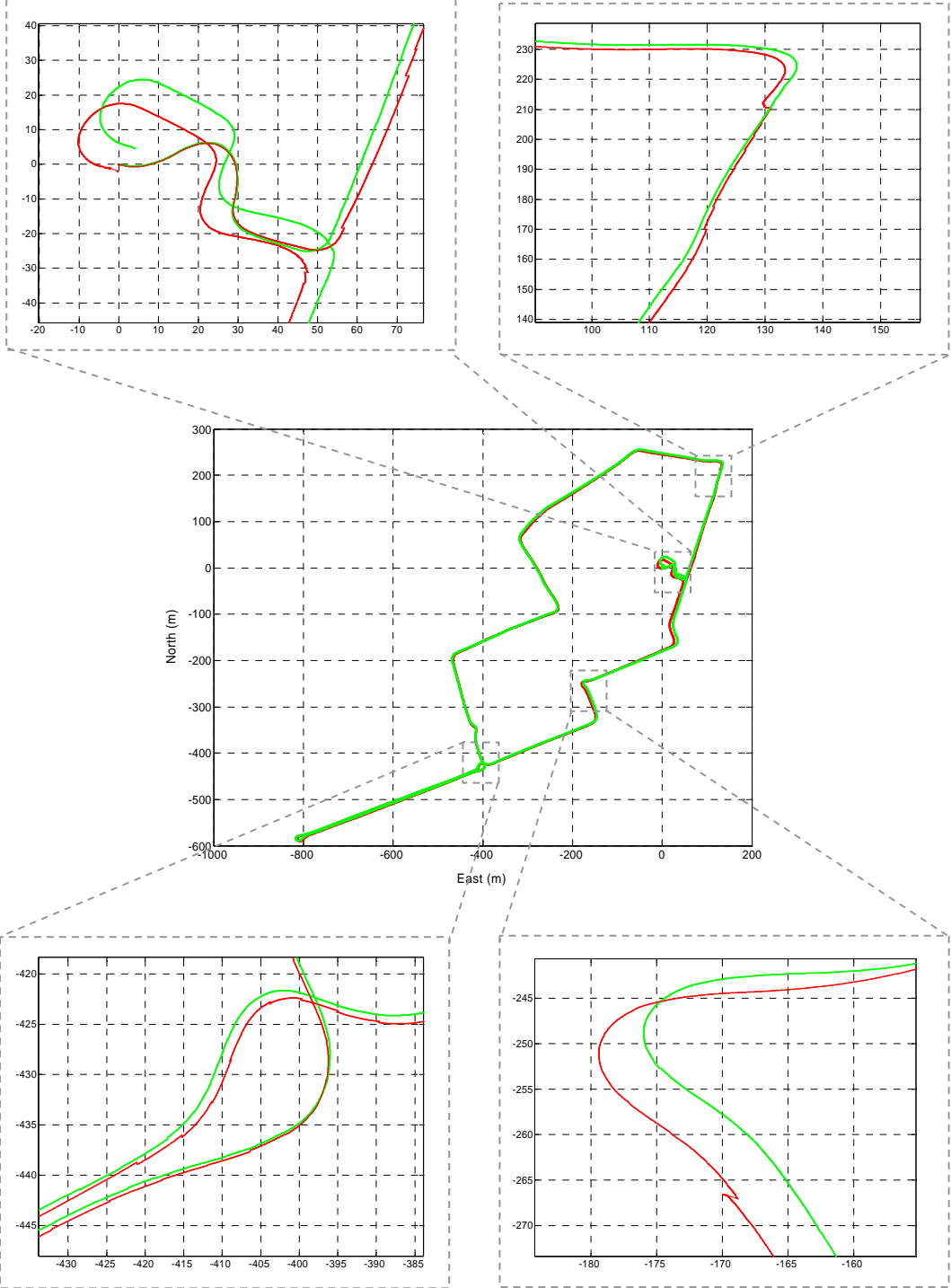


Figure 9. Horizontal position estimates from the second kinematic test dataset collected (Tightly-coupled TDCP/INS solution (*Green*) and Tightly-coupled GPS/INS solution (*Red*)).

6. CONCLUSIONS

This paper examined the performance of a tightly-coupled TDCP/INS system in an urban canyon environment. The advantage of using TDCP measurements in an urban canyon environment is that various satellites can lose lock and be reacquired without significant loss in performance provided at least four satellites are maintained between epochs. Further, the use of vehicle dynamic constraints to prevent INS error degradation during periods of GPS unavailability is also evaluated. From the results, it can be concluded that the proposed method provides an alternative ‘odometry’ solution when operating in a GPS restricted environment (e.g. DARPA Urban Challenge 2007) with the possibility of less than four GPS satellites being tracked any point in time, the pseudorange measurements are ‘contaminated’ with multipath and also without the availability of differential GPS.

REFERENCES

- Brown RG and Hagerman LL (1969), An Optimum Inertial/Doppler-Satellite Navigation System, *Journal of The Institute of Navigation*, Vol. 16, No. 3, Fall 1969.
- Brown RG and Hwang PYC (1997), Introduction to Random Signals and Applied Kalman Filtering, *New York: John Wiley and Sons, Inc. (3rd Edition)*, 1997.
- Cox DB (1978), Integration of GPS with Inertial Navigation Systems, *Journal of The Institute of Navigation*, Vol. 25, No. 2, Summer 1978.
- Chen D (1994), Development of a Fast Ambiguity Search Filter (FASF) Method for GPS Carrier Phase Ambiguity Resolution, *Ph.D. Dissertation*, The University of Calgary, Calgary, Canada.
- Farrell JL (2001), Carrier Phase Processing Without Integers, *Proceedings of Institute of Navigation 57th Annual Meeting (ION 57th AM)/CICTF 20th Biennial Guidance Test Symposium*, Albuquerque, NM.
- Ford TJ and Hamilton J (2003), A New Positioning Filter: Phase Smoothing in the Position Domain, *Journal of The Institute of Navigation*, Vol. 50, No. 2, Summer 2003.
- Goshen-Meskin D and Bar-Itzhack IY (1992), Unified Approach to Inertial Navigation System Error Modeling, *AIAA Journal of Guidance, Control and Dynamics*, Vol. 15, No. 3, 1992.
- Hatch R (1990), Instantaneous Ambiguity Resolution, *Proceedings of Kinematic Systems in Geodesy, Geomatics and Navigation (KIS) 1990*, Department of Geomatics Engineering, The University of Calgary, Calgary, Canada.
- Hofmann-Wellenhof B, Lichtenegger H and Collins J (2001), Global Positioning System: Theory and Practice, *Spinger-Verlag; Wien, New York (5th Edition)*, 2001.
- Lee HK (2004a), Integration of GPS/Pseudolite/INS for High Precision Kinematic Positioning and Navigation, *Ph.D. Dissertation*, The University of New South Wales, Sydney, Australia.
- Lee HK, Rizos C, and Jee GI (2004b), Design of Kinematic DGPS Filters with Consistent Error Covariance Information, *IEE Proceedings - Radar, Sonar and Navigation*, Vol. 151, No. 6, 2004.
- Moafipoor S, Grejner-Brzezinska DA and Toth CK (2004), Tightly Coupled GPS/INS Integration base on GPS Carrier Phase Velocity Update, *Proceedings of Institute of Navigation National Technical Meeting (ION NTM) 2004*, San Diego, California.

Soon BKH, Scheduling S and Connolly L (2006), Error Analysis of An Integrated Inertial Navigation System and *pseudoSLAM* During GPS Outages, *Proceedings of International Global Navigation Satellite Systems Society (IGNSS) Symposium 2006*, Queensland, Australia.

Soon BKH, Scheduling S, Lee HK, Lee HK, and Durrant-Whyte H (2007), An Approach to Aid INS Using Time-Differenced GPS Carrier Phase (TDCP) Measurements, *GPS Solutions* (Submitted for review).

Teunissen PJG and Tiberius CCJM (1994), Integer Least Squares Estimation of the GPS Phase Ambiguities, *Proceedings of Kinematic Systems in Geodesy, Geomatics and Navigation (KIS) 1994*, Department of Geomatics Engineering, The University of Calgary, Calgary, Canada.